Soft Matter

Cite this: *Soft Matter*, 2011, **7**, 7988

www.rsc.org/softmatter

COMMUNICATION

Microscopic origin of the terminal relaxation time in polymer nanocomposites: an experimental precedent

Klaus Nusser,*[a] Gerald J. Schneider[a] and Dieter Richter[b]

Received 31st March 2011, Accepted 4th July 2011
DOI: 10.1039/c1sm05555k

By means of rheology and neutron spin echo spectroscopy, both a macroscopic and a microscopic view on the relaxation dynamics of polymers in the presence of non-attractive nanoparticles could be realized. The results enabled us to show a direct correlation between the microscopically observed confinement length and the macroscopically measured dissipation maximum, which corresponds to the terminal relaxation time. Moreover, the impact of nanoparticle presence on the effectiveness of polymer contour length fluctuations and constraint release is discussed.

Polymer nanocomposites constitute one of the most important material classes of the present. They are frequently used in both commodity as well as high performance applications due to their high potential for tailor-made properties and functionality.[1]

Consequently the interest in a fundamental, molecular understanding of the origins of those properties is immense and numerous studies of specific polymer particle systems have been carried out. In particular, there exist uncountable studies of the rheological, calorimetric and dielectric properties of polymer nanocomposites.[2–4] From their way of approach, all these methods are of macroscopic nature, however, and can only help to understand the underlying molecular physics by way of model assumptions, which need to be evidenced. So far, no model has proven to be apt to describe all observed phenomena at once. Furthermore, both the particulate and (somewhat less often) the polymer structure in composite materials have been studied on a microscopic scale by scattering methods and transmission electron microscopy.[5] This has already helped to shed some light into the origins of material properties as well as potential mechanical reinforcement mechanisms.[6]

What has been scarcely addressed experimentally up to now, however, is a direct observation of the microscopic dynamics of long chain segments in the presence of nanoparticles. This is mainly due to the difficulty of simultaneously observing those time and length scales, which are on the order of several hundred nanoseconds and a few nanometres. Undoubtedly, however, crucial processes are very likely to occur exactly on these time and length scales. This is obvious, if one considers the dynamics of a regular entangled polymer melt. The most successful model to describe entangled polymer dynamics is the reptation model brought forth by de Gennes, where the topological confinement of a single chain by its surrounding chains is visualized by a virtual tube with diameter d_t. The impact of topological chain entanglements is a severe slowdown of the matrix relaxation, which leads to the extraordinary visco-elastic properties of bulk polymer. Typically, and depending on temperature and specific polymer type, $d_t \approx 5$ nm is found,[7,8] and the onset of entanglement constraints is visible in the segmental polymer dynamics for times in the nanosecond range.[8,9]

In the case of unfilled polymer melts, the reptation model describes also macroscopic material properties, such as linear rheology.[10,11] In the case of polymer nanocomposites, this direct correlation of microscopic and macroscopic properties is still missing. A prerequisite is a set of significant studies of the microscopic segmental dynamics in the range, where entanglement effects are active.

For unfilled polymer matrices, historically an important role in proving the assumptions of the reptation model was taken by neutron spin echo experiments, which constituted the only way to get direct microscopic insight into the polymer dynamics on the relevant length scales.[12] We have very recently shown that a similar approach is suitable to yield real microscopic information on the segmental polymer dynamics in polymer nanocomposites with non-attractive polymer particle interactions.[13] In particular, we were able to model the data by means of a reptation model with an effective confinement length or "apparent tube diameter" d_{app}, which consists of two mathematically independent contributions from the confinement by surrounding chains and by the particle structure.

In this communication, we will show that the extracted effective confinement length can be directly connected with rheological data from the same sample system. Thus, a real way to demonstrate the direct impact of microscopic changes on relevant macroscopic properties is created and highlights the need for meaningful microscopic experiments in the field in the future.

For the experiments a model nanocomposite system with non-attractive interactions was established. It was comprised of monodisperse (PDI = 1.02) poly(ethylene-*alt*-propylene) (PEP) with a molecular weight $M_w = 50$ kg mol^{-1} and spherical silica particles with a hydrophobized surface and average radius $r = 8.5$ nm. Nanocomposites with different particle volume fractions Φ were prepared by solution mixing in toluene and subsequent drying. The

[a]*Jülich Centre for Neutron Science, Outstation Garching near Munich, 85748 Garching, Germany. E-mail: k.nusser@fz-juelich.de; Fax: +49 89 289 10799; Tel: +49 89 289 10744; g.j.schneider@fz-juelich.de*
[b]*Jülich Centre for Neutron Science and Institute for Complex Solids I, 52425 Jülich, Germany*

polymer matrix in the samples consisted of protonated and deuterated PEP chains in a volume ratio 52/48, which was found to contrast match the nanoparticles. The details of the used single components as well as a detailed structural characterization including the contrast matching results and dependence of polymer dimensions and chain statistics on filler fraction were recently published in ref. 14. In brief, the chain statistics is not affected by the particle presence, whereas the chain radius of gyration is slightly reduced at high volume fractions. No signs of chain adsorption were found.

A neutron spin echo study on the sample system revealed significant changes of the segmental dynamics, when Φ was varied. This is published in detail in ref. 13. The most important result is briefly recaptured here, since it will play a crucial role in the conclusion of this communication.

In the neutron spin echo experiments the intermediate scattering function

$$S(Q,t)/S(Q) = N^{-1} \sum_{i,j} \langle \exp[-i\boldsymbol{Q}\boldsymbol{r}_i(t=0)] \exp[-i\boldsymbol{Q}\boldsymbol{r}_j(t)] \rangle$$

of the polymers is measured, where $\boldsymbol{r}_i(t)$ is the position vector of scattering center i at time t and the summation extends over all scattering centers. $\boldsymbol{Q}$ denotes the momentum transfer during the scattering event and $\langle \ldots \rangle$ is the thermal average. $S(Q,t)/S(Q)$ captures in principle a complete picture of the polymer relaxation.[12]

In Fig. 1 the intermediate scattering functions $S(Q,t)/S(Q)$ at a fixed Q value, $Q = 0.96$ nm^{-1}, are depicted for different volume fractions $\Phi \in [0; 0.6]$. The data were measured at a temperature $T =$ 150 °C at the IN15 instrument at the ILL.

The data for $\Phi = 0$ can be very well modelled by the reptation model with a tube diameter $d_t = 5$ nm, which is in agreement with existing literature on PEP (*cf.* ref. 13). For high filler fractions, the decay of $S(Q,t)/S(Q)$ is significantly slowed down. We could show in ref. 13 that this slowdown is due to an increase of the confinement rather than a change of the basic segmental relaxation rate (Rouse rate), $Wl^4(\Phi) = W_0 l_0^4$. In addition to the hindrance of the motion of a single chain by the surrounding chains, a second confinement contribution arises from the impenetrable particle structure. The two contributions can in a first approximation be replaced by one effective, total confinement length $d_{app}(\Phi)$ within the mathematical framework of the reptation theory. The extracted values for $d_{app}(\Phi)$ are given in the inset of Fig. 1, and obviously a severe decrease of the confinement length at high particle fractions takes place. The resulting $S(Q,t)/S(Q)$ from a calculation with the reptation model with confinement length d_{app} are depicted as solid lines in the figure and describe the data surprisingly well without any additional assumptions. The details of the used model can be found in ref. 13.

Now in the framework of the reptation theory, for $Wl^4 =$ const. the terminal relaxation time (disentanglement time) τ_d is directly coupled to the tube diameter *via* $\tau_d \propto d_t^{-2}$.[15] Of course, the direct microscopic observation of $\tau_d(\Phi)$ would set us in need to measure $S(Q,t)/S(Q)$ up to times $t \approx 100$ μs far away from any experimental possibility. Furthermore, the impact of contour length fluctuations (CLF) and constraint release (CR) effects is not separately included in this mean field approach, but is absorbed in the effective length d_{app}, *i.e.* d_{app} corresponds to the effective disentanglement time $\tau_{d,app}$ rather than to the bare τ_d. An examination of CLF and CR in the presence of the nanoparticles will be given later in this work.

Apart from this, it should be emphasized that for $\Phi > 0$, $\tau_{d,app}$ should more generally be called the effective, terminal relaxation time instead of disentanglement time. Regardless of this, the given relation from reptation theory enables us to give a first educated guess for $\tau_{d,app}$ by assuming

$$d_{ratio,NSE} = \frac{d_{app}(\Phi)}{d_{app}(\Phi = 0)} = \sqrt{\frac{\tau_{d,app}(\Phi = 0)}{\tau_{d,app}(\Phi)}} \quad (1)$$

In order to test this prediction, we performed oscillatory shear measurements on the same samples on an ARES rheometer from the Rheometric Scientific Company. A shear amplitude $\gamma_0 = 0.1\%$ was used and verified to be in the linear viscoelastic range for all samples. In the measurement, a sinusoidal shear rate $\gamma(t) = \gamma_0 \sin(\omega t)$ was applied and the resulting shear stress $\sigma(t) = G'(\omega)\gamma_0 \sin(\omega t) + G''(\omega)\gamma_0 \cos(\omega t)$ recorded.

In Fig. 2 an exemplary and significant snapshot of the obtained data at $T = 25$ °C is given. The loss modulus $G''(\omega)$ for three samples with $\Phi = 0$, 0.35, 0.5 is plotted with linear axes in the relevant frequency range. Note that the data of $\Phi = 0.35$ and 0.5 were shifted

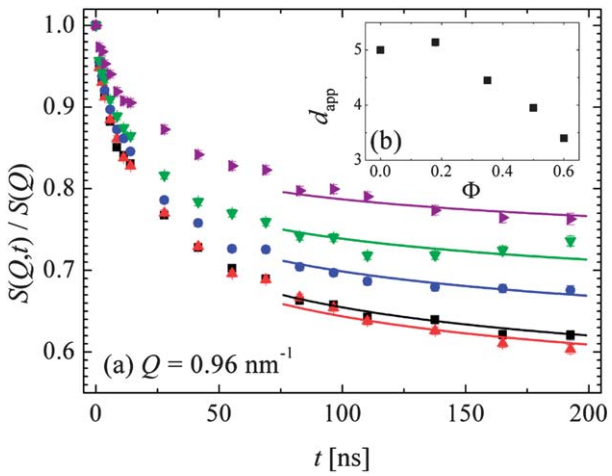

Fig. 1 (a) Intermediate scattering function $S(Q,t)/S(Q)$ at $Q = 0.96$ nm^{-1} for the filler fractions $\Phi = 0$ (■), 0.18 (▲), 0.35 (●), 0.5 (▼), 0.6 (►); solid lines are fits with the reptation model; and (b) confinement length d_{app} in dependence of Φ.

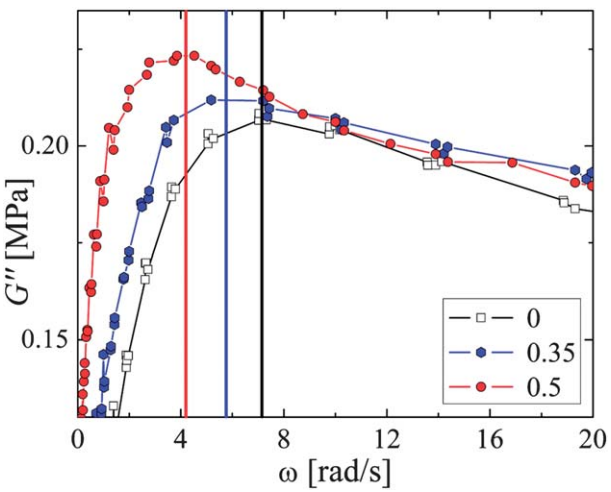

Fig. 2 Mechanical shear loss modulus $G''(\omega)$ for $\Phi = 0$ (□), 0.35 (●), 0.5 (●); the vertical lines indicate ω_{max}.

vertically for better comparison with the $\Phi = 0$ data, the vertical shift factors being 1/11 and 1/14. In this communication we will focus exclusively on the dissipation maximum. The first consideration deals with the determination of the maximum position ω_{max} of $G''(\omega)$, which is indicated by the vertical lines in Fig. 2.

In monodisperse entangled polymer melts, the position ω_{max} of the dissipation maximum is directly correlated with the inverse disentanglement time $\tau_{d,app}^{-1}$ (*e.g.* ref. 16), where $\tau_{d,app}$ is once more the effective disentanglement time, including CLF and CR. This way a similar relation to eqn (1) can be obtained:

$$d_{ratio,rheo} = \sqrt{\frac{\tau_{d,app}(\Phi = 0)}{\tau_{d,app}(\Phi)}} = \sqrt{\frac{\omega_{max}(\Phi)}{\omega_{max}(\Phi = 0)}} \quad (2)$$

Note that both eqn (1) and (2) are taken from the reptation theory for bulk polymer melts and not *a priori* applicable to the situation of polymer nanocomposites. It has been shown in ref. 13 however, that the reptation model with an effective confinement length d_{app} is able to quantitatively reproduce the experimental results. It is therefore a reasonable first approximation to assume that the reptation scaling laws are also suitable to describe the polymer dynamics in the presence of our non-attractive nanoparticles.

Thus, we are provided with a means to compare the microscopically predicted ratio of terminal relaxation times $d_{ratio,NSE}$ with the macroscopically observed one $d_{ratio,rheo}$. This comparison is illustrated for our PEP–silica system in Fig. 3.

Astonishingly, the two quantities are identical. This means that we are now in a position, where we can predict the microscopic dynamics of a nanocomposite, *i.e.* the apparent confinement length $d_{app}(\Phi)$, directly from the dissipation maximum $\omega_{max}(\Phi)$.

At this point, we want to remind the reader that in the analysis of both the rheology and of the NSE data, contour length fluctuations and constraint release were not explicitly taken into account, but implicitly absorbed in the extracted parameters. This is not a drawback with regard to the significance of our conclusions, since it is strictly consistent to compare the two effective quantities d_{app} and $\tau_{d,app}$ in NSE and rheology. Nevertheless, the examination of CLF and CR is a very important task, because it may shed even more light into the nature of the relaxation processes in the sample.

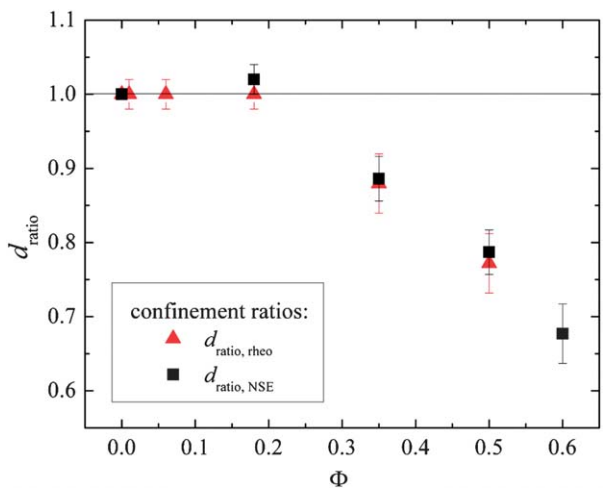

Fig. 3 Ratio of confinement lengths from rheology $d_{ratio,rheo}$ (▲) and from neutron spin echo $d_{ratio,NSE}$ (■), as calculated from the experimental data *via* eqn (1) and (2).

Moreover, in ref. 13, we already showed that the decreasing confinement length $d_{app}(\Phi)$ consists of two competing contributions. At low volume fractions Φ the confinement of a probe chain by polymer entanglements is the decisive contribution in analogy to the unfilled melt. In contrast to that, at high particle fractions the dominant confinement contribution arises from the particle structure. This is plausible, since the typical particle surface-to-surface distances are on the order of long polymer segments, and in particular at very high Φ the average surface-to-surface distance is even smaller than the undisturbed polymer tube diameter $d_t(\Phi = 0)$.

On the other hand, this perception has strong implications for the effectiveness of CR and CLF. CR relies on the notion that the tube-creating chains themselves relax and the tube is thus diluted with time. The particle structure at high Φ, however, is very immobile compared to chain segments. This should drastically diminish the effectiveness of CR. Similarly, CLF intrinsically relies on the possibility of a fluctuating chain end to forget the initial tube. This is easily achieved in a polymer matrix, where the "tube walls" are not compact, but consist of other chains with a fractal mass dimensional packing. In the case of a path confined by particles, the walls are compact particle surfaces. Small fluctuations of a chain end will lead to no additional relaxation.

With this in mind, we now return to the analysis of the rheology data and apply a more quantitative model approach. In unfilled polymer melts, it has proven successful to describe mechanical relaxation spectra by means of a phenomenological relaxation spectrum proposed by Baumgärtel, Schausberger and Winter (BSW).[17] Their ansatz is to deduce the shear modulus

$$G''(\omega) = \int_{-\infty}^{\infty} H(\tau) \frac{\omega\tau}{1 + \omega^2\tau^2} d(\ln \tau) \quad (3)$$

from a continuous logarithmic relaxation spectrum given by

$$H(\tau) = H_e\tau^{n_e} + H_g\tau^{-n_g}, \tau_0 < \tau < \tau_{max}\ H(\tau) = 0 \text{ else} \quad (4)$$

Therein, the second term describes the glassy regime at high shear frequencies and is of no relevance for the long relaxation times considered here. The first term in combination with the cutoff time τ_{max} describes the entanglement regime. In particular, τ_{max} is correlated with the disentanglement time $\tau_{d,app}$ and $-n_e$ is approximately found in the data as the right slope of the dissipation maximum in a double logarithmic plot.[18]

For pure reptation without CLF and CR, a slope $-n_e = -0.5$ is expected theoretically and found experimentally, whereas a slope $-n_e = -0.25$ is characteristic for reptation with CR and CLF.[15,18]

In Fig. 4 the rheology data of our model system are plotted on a double logarithmic scale for the volume fractions $\Phi = 0$ and $\Phi = 0.35$. The $\Phi = 0$ data can be nicely described by the BSW model and indeed a slope $-n_e = -0.16 \approx -0.25$ emerges. As expected, CLF and CR actively contribute to the relaxation.

In order to quantify the $\Phi = 0.35$ data, it is necessary to introduce a second relaxation contribution in addition to the typical polymer relaxation, given by the BSW analysis. From Fig. 4, it can be seen that there is no terminal regime of viscous flow at low ω any more. This can be attributed to the particle relaxation and is characteristic of either a percolated particle gel spanning the sample or the hindrance of the particle relaxation by a local cage. In the experimental ω window, either of the two possible particle relaxation processes can be phenomenologically described by a gel-like modulus of the form[19]

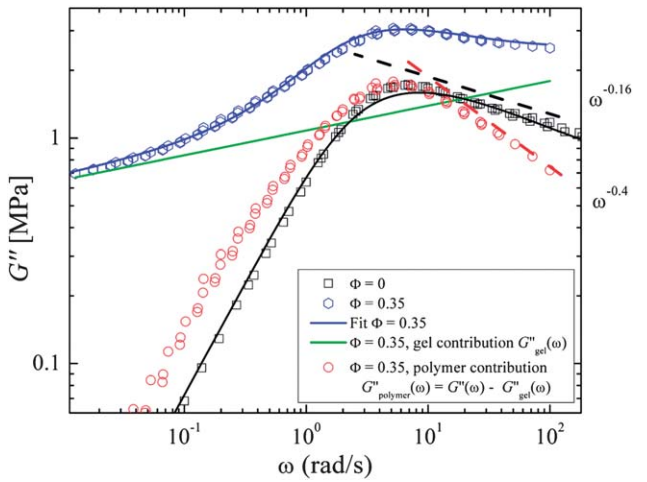

Fig. 4 Mechanical shear loss modulus $G''(\omega)$ for $\Phi = 0$ (□), 0.35 (●). The solid black and blue lines are the best fits of the $\Phi = 0$ and $\Phi = 0.35$ data. For $\Phi = 0.35$ the fit is composed of a polymer relaxation contribution and a contribution from the particle gel. The latter is indicated by the green line, the former is depicted by ●. Note that the data of $\Phi = 0$ were shifted vertically to enable a better visual comparison.

$$G_{gel}''(\omega) = const \times \omega^{n} \quad (5)$$

The observed total modulus is then a sum of the polymer contribution (eqn (3)) and the particle contribution (eqn (5)). The best fit of the $\Phi = 0.35$ data by this approach is shown in Fig. 4 as a solid blue line and yields a reasonable approximation of the experimental data $G''(\omega, \Phi = 0.35)$. It is now straightforward to extract from the nanocomposite data the polymer contribution $G_{pol}''(\omega) = G_{total}''(\omega) - G_{gel}''(\omega)$, which is also depicted in Fig. 4.

Apart from the shift of the maximum position ω_{max}, which was picked out as a central theme earlier, a change of the right slope of the dissipation maximum is obvious. For $\Phi = 0.35$, we find $-n_e = -0.40 \pm 0.15$ much closer to the bare reptation value -0.5. This observation clearly hints to a loss of importance of CR and CLF, fortifying the microscopic picture created from our NSE results that a transition from entanglement dominated towards particle dominated confinement takes place.

Similar exponents $-n_e$ in [0.25; 0.6] > 0.16 are also found for the filler fractions $\Phi = 0.18$ and $\Phi = 0.50$. We want to emphasize, however, that the statement about $-n_e$ is primarily of a qualitative nature, as indicated by the big error bar. The big uncertainty in n_e is due to the fact that the employed subtraction procedure is, of course, influenced by the determination of the gel contribution to the relaxation spectrum. The quality of the fits is satisfactory, yet not perfect, so that a certain window of acceptability for the real gel contribution has to be considered. This results in the given error on $-n_e$. Trying to extract any quantitative n_e systematics in dependence of the filler fraction is not reasonable under these preconditions and would suppose more accuracy than realistically available. The qualitative conclusions on the other hand are valid independently of the exact values of $-n_e$.

We have therefore managed to consistently correlate microscopic and macroscopic experimental evidence in a range of time and length scales, which has been barely accessed so far. In particular, all observations could be consistently integrated into the molecular picture that the chain dynamics is increasingly confined by the particle structure, whereupon the confinement is of merely topological nature. This constitutes an exciting starting point for a more complete understanding of nanocomposites with non-attractive interactions and will also have to be considered in more complex systems with attractive interactions. Moreover, the result emphasizes the role of well tailored, microscopic experimental methods such as neutron spin echo spectroscopy in combination with isotopic contrast matching in elucidating the basic physics of nanocomposites.

Acknowledgements

The authors thank L. Willner for the synthesis of the used polymers. K. Nusser gratefully acknowledges the financial support of the Evonik Foundation.

References

1 *Polymer Nanocomposites*, ed. Y.-W. Mai and Z.-Z. Yu, Woodhead Publishing Ltd., Cambridge, 2006.
2 H. Eggers and P. Schuemmer, *Rubber Chem. Technol.*, 1996, **69**, 253–265.
3 N. Hao, H. Böhning, H. Goering and A. Schönhals, *Macromolecules*, 2007, **40**, 2955.
4 J. G. Meier and M. Klüppel, *Macromol. Mater. Eng.*, 2008, **293**, 12–38.
5 S. Sen, Y. Xie, S. K. Kumar, H. Yang, A. Bansal, D. L. Ho, L. Hall, J. B. Hooper and K. S. Schweizer, *Phys. Rev. Lett.*, 2007, **98**, 128302.
6 G. Heinrich, M. Klüppel and T. A. Vilgis, *Curr. Opin. Solid State Mater. Sci.*, 2002, **6**, 195–203.
7 L. J. Fetters, D. J. Lohse, D. Richter, T. A. Witten and A. Zirkel, *Macromolecules*, 1994, **27**, 4639–4647.
8 A. Wischnewski, M. Monkenbusch, L. Willner, D. Richter and G. Kali, *Phys. Rev. Lett.*, 2003, **90**, 058302.
9 D. Richter, B. Farago, R. Butera, L. J. Fetters, J. S. Huang and B. Ewen, *Macromolecules*, 1993, **26**, 795–804.
10 A. E. Likhtman and T. C. B. McLeish, *Macromolecules*, 2002, **35**, 6332–6343.
11 M. Abdel-Goad, W. Pyckhout-Hintzen, S. Kahle, J. Allgaier, D. Richter and L. J. Fetters, *Macromolecules*, 2004, **37**, 8135–8144.
12 D. Richter, M. Monkenbusch, A. Arbe and J. Colmenero, *Adv. Polym. Sci.*, 2005, **174**, 1.
13 G. J. Schneider, K. Nusser, L. Willner, P. Falus, and D. Richter, *Macromol.*, 2011DOI: 10.1021/ma200899y.
14 K. Nusser, S. Neueder, G. J. Schneider, M. Meyer, W. Pyckhout-Hintzen, L. Willner, A. Radulescu and D. Richter, *Macromolecules*, 2010, **43**, 9837–9847.
15 M. Rubinstein and H. C. Colby, *Polymer Physics*, Oxford University Press, Oxford, 2007.
16 J. D. Ferry, *Viscoelastic Properties of Polymers*, Wiley, New York, 1980.
17 M. Baumgärtel, A. Schausberger and H. H. Winter, *Rheol. Acta*, 1990, **29**, 400.
18 M. Abdel-Goad, W. Pyckhout-Hintzen, S. Kahle, J. Allgaier, D. Richter and L. J. Fetters, *Macromolecules*, 2004, **37**, 8135.
19 H. H. Winter and F. Chambon, *J. Rheol.*, 1986, **30**, 367.